

# Composition of Anomalous Cosmic Rays and Other Ions from Voyager Observations

A.C. Cummings, E.C. Stone, and C. D. Steenberg

Space Radiation Laboratory, Caltech, MC 220-47, Pasadena, CA 91125, USA

## Abstract

We present energy spectra of eleven cosmic ray elements with energies from  $\sim 5$  to  $\sim 500$  MeV/nuc using data obtained from the Voyager spacecraft in the outer heliosphere from early 1993 to the end of 1998. The low-energy intensity increases observed in all these spectra are consistent with the shapes expected to be exhibited by primarily singly-charged anomalous cosmic rays (ACRs). One of these elements is Na, which is being reported as a member of the ACR component for the first time. We find that the intensity increase below  $\sim 10$  MeV/nuc in the Si spectrum in the outer heliosphere is not dominated by re-accelerated solar wind. There is also evidence for a non-ACR component in the energy spectra of Mg, Si, and S observed at 1 AU by the Wind spacecraft below  $\sim 5$  MeV/nuc. We see evidence in the energy spectra of Ar in both the inner and outer heliosphere for multiply-charged ACRs above  $\sim 360$  MeV. Using a fit to the ACR intensities with a full-drift, two-dimensional numerical model of the acceleration and propagation of singly-charged ACRs, we present a table of the relative abundances of the seed particles of eleven elements at the solar wind termination shock.

## 1 Introduction:

Anomalous cosmic rays (ACRs) are traditionally defined as those particles in the energy spectra of cosmic rays which originated as interstellar neutral gas and which became ionized and accelerated in the heliosphere (Fisk et al. 1974). Most of the characteristic increase in intensity of ACRs at low energies is due to singly-charged particles (Klecker et al. 1995), although at the higher-energy portion of the ACR spectrum there may be a significant contribution from multiply-charged particles (Mewaldt et al. 1996).

In the outer heliosphere, the well-established members of this component are H, He, C, N, O, Ne and Ar (Cummings & Stone 1998). At 1 AU, recent observations with the Wind spacecraft have revealed intensity increases at low energies of other ions, such as Mg, Si, and S (Reames 1999), the latter two of which were also observed in the outer heliosphere (Stone & Cummings 1997). The origin of these low-energy intensity increases is not clear, having been attributed to the ACR component (Stone & Cummings 1997), as well as to re-accelerated solar wind (Mewaldt 1999).

## 2 Observations:

In Figure 1 we show the energy spectra acquired during 1993/53 - 1998/365 at V1 and V2 for H, He, C, N, O, Ne, Na, Mg, S, and Ar. All of the energy spectra show an increase at low-energies. In the case of H, the ACR component peaks at  $\sim 40$  MeV, with an additional increase below  $\sim 5$  MeV that is likely due to a local interplanetary acceleration process. Also shown in Figure 1 are model calculations of singly-charged ACRs from a full-drift, two-dimensional model using the same parameters (except for intensity normalization) as used to fit the 1998 data in the outer heliosphere (Steenberg et al. 1999).

The calculated ACR curves for each element were fit to the ACR intensities at V1 and V2 simultaneously. The ACR intensities were derived from the observations by subtracting a galactic cosmic ray (GCR) component which was assumed to be a power law in energy/nuc with index 0.8 and with an intensity adjusted to match the high-energy portion of the observed energy spectra. Curves representing the sum of the ACRs and GCRs match the observations reasonably well.

In Figure 2a we show data and model curves for Si, similar to those shown in Figure 1. In this case, the sum of the model ACR curve and the power-law GCR spectrum was fit to the data, with two free parameters to set the GCR intensity levels at V1 and V2, respectively, and a third to set the overall ACR level. The observations show a clear increase in intensity below  $\sim 10$  MeV/nuc at both V1 and V2.

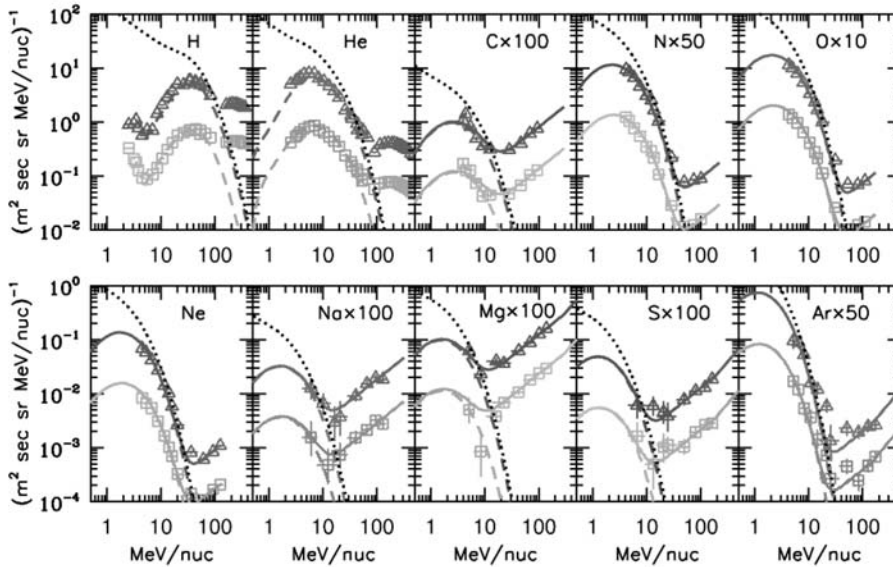


Figure 1: Energy spectra of 10 elements at V1 (triangles) and V2 (squares) for 1993/53-1998/365 from the CRS experiment. In some panels factors are shown which have been applied to the V1 observations before plotting. The V2 observations use the same factors for V1 plus an additional factor of 0.2 for clarity purposes. The dashed curves are model calculations using the model and parameters from Steenberg et al. (1999), except for the intensity normalization, which is described in the text. The dotted curve is the spectrum at the shock at a polar angle of  $60^\circ$ . The solid curves are the sum of ACRs and GCRs as described in the text.

### 3 Discussion:

The increases at low energies ( $\lesssim 100$  MeV/nuc for H and He and  $\lesssim 10$ -30 MeV/nuc for the other elements) are reasonably consistent with the model calculations which assume the ions are singly-charged ACRs. In Figure 2b we show the Si observations at V1 and V2 along with best-fit model calculations assuming the Si charge state is +8.6, used by Mewaldt (1999) to suggest that re-accelerated solar wind could be responsible for the low-energy intensity increases of Si, S, and Fe (not addressed here) in the outer heliosphere. The  $\chi^2$  of the fit is 27.0 for 15 degrees of freedom, indicating a probability of  $\lesssim 3\%$  that the observations are consistent with the model spectra with  $Q=8.6$ . The  $\chi^2$  of the fit in Figure 2a is 14.6 for 15 degrees of freedom, indicating consistency of the low-energy increases in the spectra of Si at V1 and V2 with the model ACR spectra with  $Q=1$ .

To address the question of the origin of the intensity increases at low energy reported by Reames (1999) for Mg, Si, and S, we have compared the spectral shapes of these elements to that of a well-known ACR component, Ne, in Figure 3. We also compare the spectral shapes of two ACR components that bracket the mass range of the three mentioned above by showing in Figure 3a the ratio of Ar to Ne intensities. Data from 1 AU from the Wind spacecraft (Reames 1999) are shown after subtracting a GCR contribution to the observed intensities. The high-energy portion of the energy spectra were used to determine the coefficients of the power laws in energy/nuc assumed for the GCRs. The power-law index was fixed at 0.8. The same subtraction technique was used for the Voyager data.

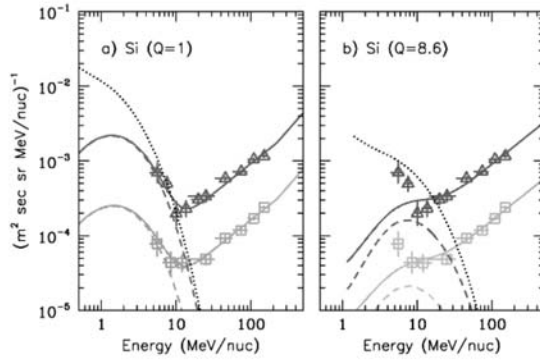


Figure 2: a) Energy spectra of Si at V1 (triangles) and V2 (squares) for 1993/53-1998/365 from the CRS experiment. The curves are similar to those in Figure 1, except the normalization of the GCR and ACR intensities was achieved by a fit to the observed intensities. The V2 points and curves are multiplied by 0.2 before plotting. b) Same as a) except the model calculations assume the charge state of Si is +8.6, typical of the solar wind.

The ACR Ar/Ne ratios observed at 1 AU and at V1 and V2 are all consistent with the expected ratios from the model calculations of Steenberg et al. (1999) below  $\sim 10$  MeV/nuc. The curve shown in Figure 3a assumes that the ions are singly-charged. Above  $\sim 10$  MeV/nuc ( $\sim 360$  MeV for Ar), it appears that the Ar intensities at both 1 AU and in the outer heliosphere significantly exceed the expected intensities from singly-charged ACRs, suggesting that the excess is due to doubly-charged ions (and perhaps higher charge states, as well), as expected from theory (Jokipii 1996) and SAMPEX observations at 1 AU (Mewaldt et al. 1996). A contribution from multiply-charged ACRs may also explain the excess in the S/Ne ratio above 10 MeV/nuc in Figure 3b.

There is also reasonable agreement among the observations at 1 AU and at V1 and V2 of S/Ne, Si/Ne, and Mg/Ne above  $\sim 5$  MeV/nuc. The ratios at these energies also agree with the model calculations. However, at lower energies ( $< 5$  MeV/nuc for S and  $< 4$  MeV/nuc for Si and Mg) the observations at 1 AU exceed the model calculations by factors of 1.7 to 5. This indicates that the 1 AU spectra for S, Si, and Mg are steeper than either Ne or Ar. Since at the same low energies, the Ar/Ne ratio (Figure 3a) agrees so well with the model calculations for ACRs with  $Q=1$ , this suggests that there is an additional, non-ACR contribution to the lowest energy 1 AU fluxes.

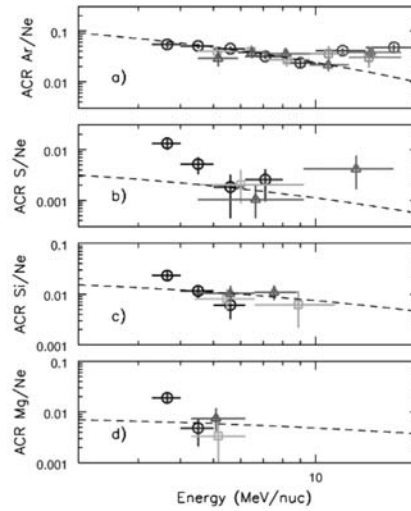


Figure 3: Intensity ratios of Ar, S, Si, and Mg ACRs to ACR Ne at 1 AU (circles), V1 (triangles), and V2 (squares). The dashed lines are the ratios from the model calculations of Steenberg et al. (1999) at V2 assuming the ions are singly-charged.

The dotted curves in Figures 1 and 2a represent the expected intensities of ACRs at the solar wind termination shock at a polar angle of  $60^\circ$ , near the average polar angles of the observations, which were  $33^\circ$  and  $14^\circ$  for V1 and V2, respectively. As can be seen from Figure 1, for the parameters used in the model, the power-law portion of the shock spectrum occurs at energies below those observed. Because the observed energies correspond to the roll-off region of the shock spectrum, the observed abundances do not directly correspond to the abundances of the injected seed particles. This can be seen in both the observed and model energy dependence of Ar/Ne in Figure 3a. However, at lower energies ( $\lesssim 1$  MeV/nuc), the ACR source abundances are reflected in the relative intensities of the power-law portions of the shock spectrum. The ACR source abundances in Table 1 were determined from the intensities at the shock in Figures 1 and 2a at 0.5 MeV/nuc.

Also shown in Table 1 are the ACR source abundances derived by Reames (1999) using a force-field model to fit the 1 AU spectra. The larger abundances of Mg, Si, and S (factors of 2.5, 1.7, and 2.8, respectively) inferred from the 1 AU observations reflect the possible presence of a non-ACR component as discussed above. The smaller abundances of Ar inferred from the 1 AU data, however, results from differences in the force-field and the 2-D drift model fits, since the observations at 1 AU, V1, and V2 are consistent. In particular, the force-field model assumes that a power-law source spectrum extends to the observed energy interval, while the self-consistent 2-D drift model exhibits a non-power law roll off above  $\sim 1$  MeV/nuc, as discussed above. As a result, the fits reported here should provide an improved estimate of the ACR source abundances.

Table 1: Abundances of ACRs (Relative to O) at the Solar Wind Termination Shock

Element	This work	Reames (1999)
H	$(1.22 \pm 0.07) \times 10^1$	-
He	$6.27 \pm 0.36$	$5.00 \pm 0.50$
C	$(6.25 \pm 0.74) \times 10^{-3}$	$< 1.00 \times 10^{-2}$
N	$(1.39 \pm 0.09) \times 10^{-1}$	$(1.20 \pm 0.10) \times 10^{-1}$
O	1.00	$1.00 \pm 0.01$
Ne	$(7.25 \pm 0.44) \times 10^{-2}$	$(7.0 \pm 0.7) \times 10^{-2}$
Na	$(1.57 \pm 0.63) \times 10^{-4}$	$< 2.0 \times 10^{-4}$
Mg	$(4.71 \pm 2.03) \times 10^{-4}$	$(1.2 \pm 0.3) \times 10^{-3}$
Si	$(9.99 \pm 2.05) \times 10^{-4}$	$(1.7 \pm 0.3) \times 10^{-3}$
S	$(2.15 \pm 1.01) \times 10^{-4}$	$(6.0 \pm 2.0) \times 10^{-4}$
Ar	$(6.40 \pm 0.65) \times 10^{-3}$	$(4.2 \pm 0.5) \times 10^{-3}$

**Acknowledgments:** We thank E. Christian for algorithms to analyze the H and He events which do not stop within the CRS detectors (e.g.,  $\gtrsim 80$  MeV/nuc). This work was supported by NASA under contract NAS7-918.

## References

- Cummings, A. C. & Stone, E. C. 1998, *Space Sci. Rev.*, 83, pp. 51–62  
 Fisk, L. A., Kozlovsky, B., & Ramaty, R. 1974, *Astrophys. J. Lett.*, 190, pp. L35–L38  
 Jokipii, J. R. 1996, *Astrophys. J. Lett.*, 466, pp. L47–L50  
 Klecker, B., McNab, M. C., Blake, J. B., et al. 1995, *Astrophys. J. Lett.*, 442, pp. L69–L72  
 Mewaldt, R. A. 1999, *Adv. Space Res.*, in press  
 Mewaldt, R. A., Selesnick, R. S., Cummings, J. R., et al. 1996, *Astrophys. J. Lett.*, 466, pp. L43–L46  
 Reames, D. V. 1999, *Astrophys. J.*, in press  
 Steenberg, C. D., Cummings, A. C., & Stone, E. C. 1999, in *Proc. 26th Internat. Cosmic Ray Conf.*, SH 4.4.03, Salt Lake City  
 Stone, E. C. & Cummings, A. C. 1997, in *Proc. 25th Internat. Cosmic Ray Conf.*, 2, pp. 289–292, Durban